Nanofluidic Diodes Based on Nanotube Heterojunctions

ARTICLE *in* NANO LETTERS · AUGUST 2009

Impact Factor: 13.59 · DOI: 10.1021/nl9020123 · Source: PubMed

4 AUTHORS, INCLUDING:

Ruoxue Yan
University of California, Berkeley
19 PUBLICATIONS **2,720** CITATIONS
SEE PROFILE

Wenjie Liang
Chinese Academy of Sciences
30 PUBLICATIONS **4,684** CITATIONS
SEE PROFILE

NANO LETTERS

2009
Vol. 9, No. 11
3820-3825

Nanofluidic Diodes Based on Nanotube Heterojunctions

Ruoxue Yan,† Wenjie Liang,† Rong Fan, and Peidong Yang*

Department of Chemistry, University of California, Berkeley, California 94720, and Materials Science Division, Lawrence Berkeley National Laboratory, Berkeley, California 94720

Received June 23, 2009; Revised Manuscript Received July 8, 2009

ABSTRACT

The mechanism of tuning charge transport in electronic devices has recently been implemented into the nanofluidic field for the active control of ion transport in nanoscale channels/pores. Here we report the first synthesis of longitudinal heterostructured SiO_2/Al_2O_3 nanotubes. The ionic transport through these nanotube heterojunctions exhibits clear current rectification, a signature of ionic diode behavior. Such nanofluidic diodes could find applications in ion separation and energy conversion.

Semiconductor diodes and field effect transistors have laid the foundation for the modern electronic and optoelectronic industry. The mechanism of tuning charge transport in electronic devices has recently been implemented into the nanofluidic field for the active control of ionic transport in nanoscale channels/pores.[1−10] These artificial nanochannel/pore devices often passively transport ionic species, similar to simple electron transport in a *resistor*. Introducing an external electrical field to modulate ionic conductivity in nanoscale channels has resulted in p- and n-channel nanofluidic *transistors* which exhibit rapid modulation of ionic conductance.[11−13] It was also being proposed that "pn-junction diode" type nanochannels could function as nanofluidic *diodes* and bipolar transistor diodes.[14] Realization of such nanofluidic diode devices should represent a significant step toward building ionic equivalents of electron devices and integrate circuits. They would also lead to novel ion separation and energy conversion technologies, due to their unique ion transport properties.[15−17] Although this concept has recently been demonstrated in molecular junctions,[18,19] and asymmetric channels made through diffusion limited patterning,[20−22] solid-state nanofluidic diodes based on intrinsic pn ionic junctions have not been demonstrated due to difficulty in designing and fabricating nanotube heterojunctions with opposite surface charge type. Here we report the first synthesis of longitudinal heterostructured SiO_2/Al_2O_3 nanotubes. The ionic transport through these nanotube heterojunctions exhibits clear current rectification, a signature of ionic diode behavior.

Nanofluidics is attracting increasing attention recently as the dimensions for chemical and biological analytical techniques are being scaled down in order to achieve ultrasensitive or even single molecule level detection. For nanofluidic channels with dimensions smaller than the characteristic length scale for ion screening known as Debye length (λ_D), overlapping of electric double layers of charged channel walls results in a unipolar solution of counterions.[23,24] The Debye length, $\lambda_D \propto I^{-1/2}$, I being the total ionic strength, usually ranges between 1 and 100 nm in aqueous solution. In a unipolar environment, the average concentration of the counterions in a nanotube with radius r is dictated by electroneutrality and depends on the surface charge density σ of the channel wall: $C = 2|\sigma|/rF$, F being the Farady Constant. The polarity of the counterions depends on the type of surface charge on the channel. Negative surface charges would yield cation majority carriers in the channel, and vice versa. For example, we have previously demonstrated that surface functionalization within silica nanotubes can switch the nanofluidic transistors from *p-type* field effect nanofluidic transistors, to *n-type* field effect transistors.[12]

A nanotube hetetojunction with opposite surface charges on two segments of the channel walls should in principle function as an ionic diode to rectify the ion current. This ionic analogue of a semiconductor p−n junction could find its origin in "bipolar membranes"[25−27] where oppositely charged ion-exchange membranes were put in physical contact. Introducing such "pn-junction" type nanochannels in fluidic systems has led to the proposal of nanofluidic diodes and bipolar junction transistors (BJTs).[14] The diode behavior has recently been observed in channels that are chemically or geometrically asymmetric.[20,21] These early demonstrations have been made possible through surface functionalization of the selected segments within the same single nanochannel. No nanofluidic diodes, however, have

† These authors contribute equally to this work.

10.1021/nl9020123 CCC: $40.75
Published on Web 07/15/2009

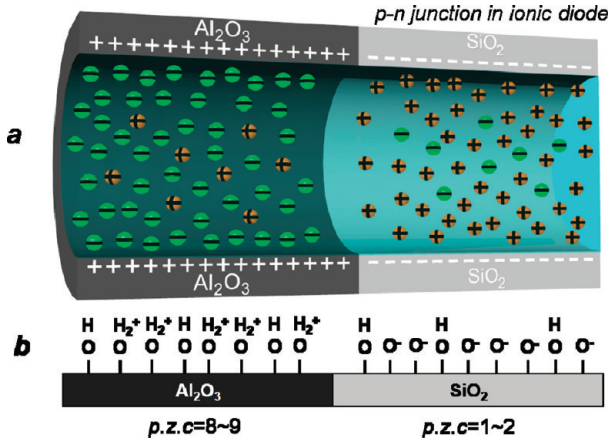

Figure 1. Schematics of a nanotube heterojunction. (a) Schematic illustration of ion distribution in a nanoionic diode consisting of longitudinally heterostructured oxide nanotube. (b) Inner surface structure of a nanofluidic diode. It shows the origin of the opposite surface charges on the inner surface of the tube at neutral or mild acidic pH values.

been demonstrated so far based on intrinsic pn-junction ionic channel.

It has been demonstrated previously that SiO_2 nanotubes serve as the *p-type* ionic channel in which the majority charge carriers are cations in the unipolar region.[12,13] This is based on the surface chemistry of the metal oxide surface in contact with an aqueous solution and is determined by the dissociation of the hydroxyl groups. The general equilibrium can be expressed as: $M-OH_2^+ \rightarrow M-OH + H^+ \rightarrow M-O^- + 2H^+$, which shifts to the right as pH increases. For each oxide surface, there exists a pH value known as point of zero charge (p.z.c.), where the surface hydroxyl groups are undissociated and the surface has zero net charge. This p.z.c. value depends on the electronic nature of the metal−oxygen bond and the stoichiometry of the surface. The SiO_2 surface has a p.z.c. of 1−2,[28] so the surface carries net negative surface charge at neutral pH. Al_2O_3, on the other hand, has a p.z.c. of 8−9,[28] which means at pH = 7 the surface chemistry is dominant by $Al-OH + H^+ \rightarrow Al-OH_2^+$, and the surface carries a net positive surface charge. Hence an Al_2O_3 nanotube will behave as an n-type nanofluidic channel, which allows the transport of anionic majority species under unipolar condition. A longitudinal, heterojunctioned nanotube, with half of the tube being SiO_2 and the other half Al_2O_3, if it can be made, should function as a pn ionic diode and exhibit ionic current rectification (Figure 1).

We have designed and successfully synthesized the proposed Al_2O_3/SiO_2 heterojunction nanotube as the target building block for nanofluidic p−n diodes. A synthetic strategy toward Al_2O_3/SiO_2 heterojunction nanotubes was developed, using silicon nanowires as templates and a simple fabrication process to integrate single nanotube fluidic channels into a nanofluidic diode device. The synthetic procedure of heterostructured Al_2O_3/SiO_2 nanotubes is schematically illustrated in Figure S1 in the Supporting Information. With vertical silicon nanowire arrays as templates,[29] heterojunction SiO_2/Al_2O_3 nanotube arrays can be made through multiple steps of conformal atomic layer deposition (ALD), protection/deprotection, and selective etching.

Figure 2a shows the scanning electron microscope (SEM) image of vertical $Si-SiO_2/Al_2O_3$ nanowire array on a Si(111) substrate. The bottom halves of the Si nanowires are conformally coated with Al_2O_3 by atomic layer deposition, while the top halves are pure Si nanowire whose original Al_2O_3 coating has been selectively removed by wet etching. A sharp diameter modulation is clearly visible at the junction. The transmission electron microscope (TEM) image (Figure 2b) of the final heterojunction oxide nanotubes after removal of the Si core also shows a distinct wall thickness contrast at the junction. The thinner part of the tube consists of pure SiO_2, whereas the thicker part is a coaxial core−shell structure of Al_2O_3/SiO_2 wall with Al_2O_3 being the inner wall. The nanotubes, though having a sharp modulation in the wall thickness at the Al_2O_3/SiO_2 junction, form a smooth and homogeneous inner surface throughout the lengths of the nanotubes, as can be seen in the close-up scanning TEM image in Figure 2c (left). EDAX elemental mapping (Figure 2c, right panel) gives explicitly the distributions of Al, Si, and O elements over this junction. The dashed line outlined the shape of the heterojunction. It can be seen that Al atoms (top graph, Figure 2c, right panel) only exist at the upper section of the junction and only on the inner layer (~30 nm) of the nanotube wall. There is no Al signal from either the outer layer or the whole lower section of the junction. Si signals (middle, Figure 2c, right panel) appear on both sections. For the upper half, Si only resides in the ~50 nm thick outer layer, closely wrapping around the Al-abundant shell. For the lower half of the junction, the tube wall is composed exclusively of Si and O. This mapping result shows unambiguously that the inner surfaces of the as-made nanotubes are indeed half Al_2O_3 and half SiO_2 with distinct heterojunctions formation as designed.

The inherent charge discontinuity for the inner surface of the as-made heterojunction nanotubes was first confirmed by fluorescent mapping with ionic dyes selectively absorbed inside the nanotubes. To visualize the surface charge polarity in the Al_2O_3/SiO_2 heterojunction nanotubes, we introduced two fluorescent dyes that carry opposite charges in neutral pH: Fluorescein and Rhodamine 6G (R6G). Fluorescein and Rhodamine 6G are both laser dyes with high quantum yield and high photostability in aqueous solution. Fluorescein is a weak carboxyl acid with $pK_a = 3.31$.[30] At neutral pH, it carries a negative charge which can bind selectively to the positively charged Al_2O_3 surface through electrostatic interaction. On the contrary, Rhodamine 6G (R6G) has an amino group that is protonated at neutral pH and bears a positive charge that can be absorbed selectively onto the negatively charged SiO_2 surface. Should there be a switch in surface charge polarity in the Al_2O_3/SiO_2 heterojunction nanotubes, the two types of charged dye molecules in a low ionic strength environment would selectively diffuse into and reside in the segment of the nanotubes with opposite surface charges. Consequently, the surface charge on the Al_2O_3 and SiO_2 segments of the nanotubes could be distinguished optically by the distinct fluorescent emissions of the two dyes.

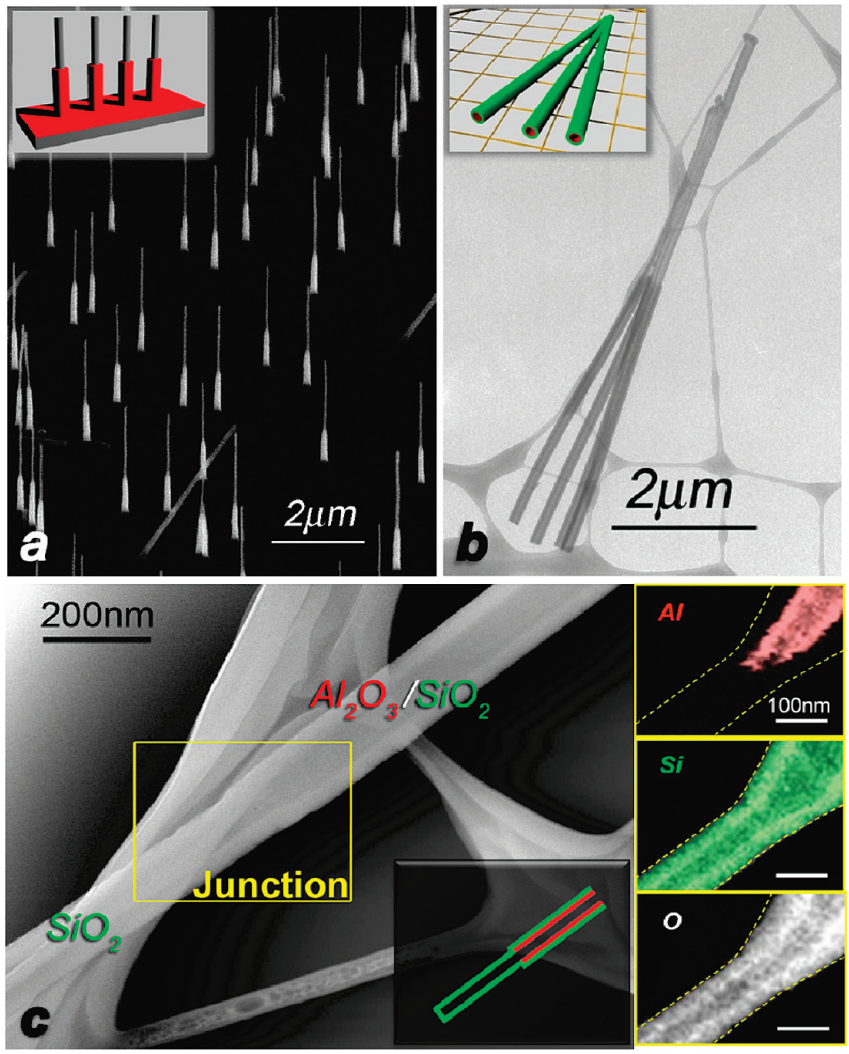

Figure 2. Electron micrographs of the heterojunction nanotubes. (a) SEM image of Si−Si/Al_2O_3 nanowire array on Si(111) substrate (Inset: cartoon of the nanowire array). (b) Representative TEM image of diode nanotubes (Inset: cartoon of the diode nanotubes on a TEM grid). (c) STEM picture of a single SiO_2/Al_2O_3 junction on a heterostructure nanotube and the elemental mapping of Al, Si, and O on the junction (right panels) (Inset: cartoon of the cross section of a heterojunction nanotube).

The feasibility of probing surface charge polarity with charged dye molecules was first demonstrated with pure SiO_2 and Al_2O_3 nanotubes. The dye loading procedure is so designed to ensure a unipolar environment within the nanotubes: 10 μL of 10 mM dye solution was dropcasted on pure SiO_2 or Al_2O_3 nanotubes supported on a fused silica substrate. Under this ionic strength, the Debye screening length at the metal oxide surface was about 3 nm, and surface charges were completely shielded by counterions once diffusion equilibrium is reached, so that the concentration of dye ions in the nanotube was dictated by bulk concentration. The nanotubes were then washed 3 times in 20 mL of deionized water bath for 5 min each time to reduce the bulk dye concentration and the ionic strength, so that the system moves into a unipolar condition. After this step, the fluorescent background from the bulk solution was suppressed/eliminated, and the counterion concentration inside nanotubes became governed by the surface charge density of the nanotubes and co-ions are expelled from the nanotubes. The wet quartz substrate with dye-loaded nanotubes was then capped with a quartz coverslip for imaging.

The fluorescence measurement setup is shown in Figure 3a. The excitation laser was brought in from the side and focused on the nanotubes. The fluorescent signals from the absorbed dyes are collected by a 50× objective and captured by an ultrasensitive CCD camera. Incident excitation beam scattered off the sample was blocked by notch filters of the corresponding laser wavelengths. Figure S3 in the Supporting Information shows the fluorescent images from pure SiO_2 and Al_2O_3 nanotubes loaded with either R6G or Fluorescein under 442 nm laser excitation. Only SiO_2 nanotubes loaded with R6G and Al_2O_3 nanotubes loaded with Fluorescein showed fluorescence that outlines the shape of nanotubes, whereas SiO_2 nanotubes loaded with Fluorescein and Al_2O_3 nanotubes loaded with R6G remained dark. This result confirmed that SiO_2 and Al_2O_3 carry opposite surface charges under neutral pH.

To demonstrate the surface charge discontinuity in heterojunction nanotubes, cationic R6G and anionic Fluorescein was subsequently loaded into the SiO_2/Al_2O_3 nanotubes and washed/diluted using the method described above. A dual laser excitation (He:Cd laser at 442 nm and Nd:YAG laser

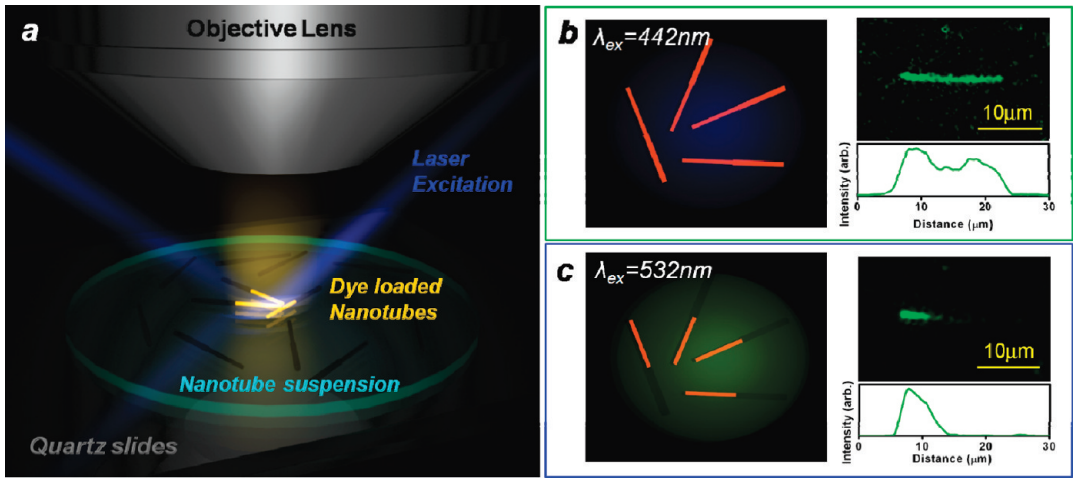

Figure 3. Optical imaging of ion distribution in heterojunction nanotubes. (a) Schemetic of the fluorescence measurement setup. (b and c) Fluorescent micrographs and intensity profiles of a single diode nanotube loaded with fluorescent dye molecules with opposite net charges (R6G with net positive charges and fluorescin with net negative charges) under 442 nm laser excitation (b) and 532 nm laser excitation (c), respectively.

at 532 nm) was used to distinguish the emissions from the two laser dyes. R6G fluorescence can be effectively excited at both 442 and 532 nm, whereas Fluorescein has an absorption cutoff at 520 nm, and can only be excited at 442 nm. Figure 3b shows the fluorescent images of a single 15 μm long heterojunction nanotube under different excitation wavelengths. The upper image was collected when the nanotube was illuminated at 442 nm. Both Fluorescein and R6G showed strong fluorescence, outlining the entire nanotube. The lower image was collected when the nanotube was excited by 532 nm laser. Here only R6G was excited and only the SiO_2 half of the nanotube was lit up. The fluorescence intensity profile along the length of the nanotube also showed an abrupt intensity drop to the background level in the middle of the nanotube, where the heterojunction was expected. This segmented emission confirmed the surface charge polarity switch within the nanotube as designed.

Nanofluidic diode devices interfaced with microfluidic channels (Figure 4a) were fabricated using a modified procedure. Si nanowires, which will later template the diode nanochannel, were grown laterally from the side wall of microtrenches that were prefabricated on silicon-on-insulator (SOI) wafer according to a well-established procedure developed in our group (Figure S3a in the Supporting Information).[31] Using this wire-in-trench design, wire growth can be directly integrated into device fabrication to significantly simplify the fabrication procedures. SEM images of a single bridging Si nanowire at different stages of fabrication are given in Figure S4a−c in the Supporting Information. Figure 4b is an optical image showing the structure of the final diode device while it was being filled by deionized water. This final nanofluidic device consists of a heterojunction SiO_2/Al_2O_3 nanotube connected by two large microfluidic reservoirs at the both ends.

Previously we have demonstrated that silica nanotubes can serve as p-channel nanofluidic transistors because of their intrinsic negative surface charges.[13] Similarly, alumina nanotubes should serve as n-channel nanofluidic transistors because

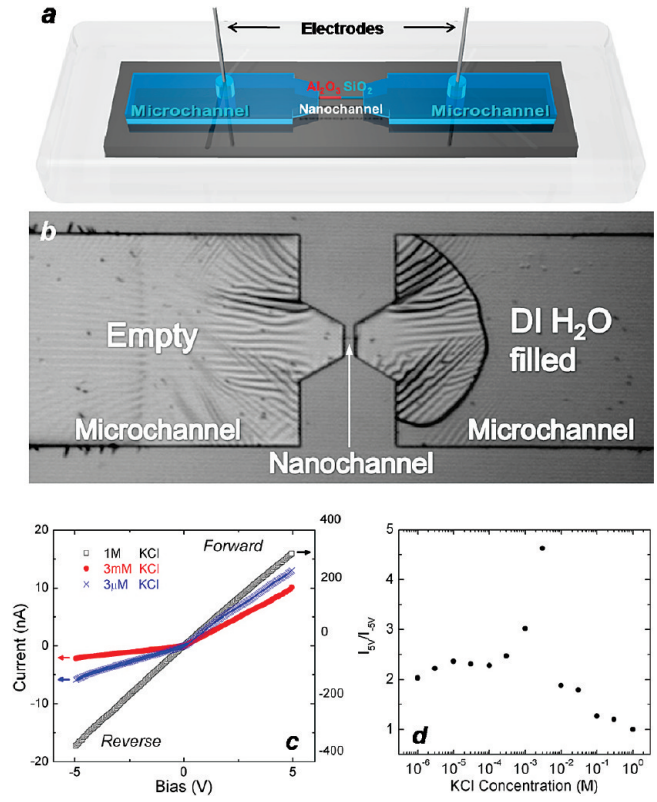

Figure 4. Nanofluidic diode device and current rectification behavior of a single nanotube diode. (a) Schematic of the nanotube diode device. (b) Optical micrograph of a nantube diode device being filled by deionized water. (c) Current rectification of the nanotube diode under high (1 M), medium (3 mM), and low (3 μM) KCl concentration at neutral pH. (d) Current ratio of the forward and reverse direction at 5 V/−5 V at different KCl concentrations.

of their intrinsic positive surface charges. Figure S5 in the Supporting Information shows the measured ionic conductance of pure Al_2O_3 nanotube devices measured at different concentrations of KCl solution under low bias voltage. It shows unipolar characteristics that deviate from the bulk behavior at low concentrations, which confirm surface-charge

governed transport, consistent with the SiO_2 nanotube devices reported previously.[13] The surface charge density can be estimated from the ionic current in the unipolar transport region. It has been demonstrated previously that a SiO_2 nanochannel has a surface charge density of $0.01-0.1 C/m^2$.[13] Measurement on pure Al_2O_3 nanotube indicated the ALD grown Al_2O_3 film has a surface charge density of $\sim 0.1\ C/m^2$, consistent with reported values of positively charged Al_2O_3 surfaces.[32,33] It should be noted that this value is comparable to that of SiO_2 nanochannels, only with opposite polarity.

Experimental $I-V$ curves obtained at different KCl concentration in the ± 5 V bias range show ionic strength dependent ionic current rectification behavior (Figure 4c). At high KCl concentration (Figure 4c, open diamond), no diode characteristic is observed. This is because under such high ionic strength, $C_{bulk} \gg 2|\sigma|/rF$, the Debye layer is compressed to within 1 nm and the surface charge is completely shielded by the counterions. The surface charge effect on ionic transport becomes negligible, bipolar ionic transport dominates, and no current rectification behavior is expected. At low ionic strength, the Debye length becomes comparable with the nanotube dimension, and the surface effect becomes prominent. Without applied bias along the channel, K^+ ions accumulate in the SiO_2 segment of the nanotube to compensate for the negative surface charge as required by electroneutrality, whereas Cl^- ions enrich in the Al_2O_3 half. As a positive voltage bias is applied, both K^+ and Cl^- inside the electric double layer are driven toward the junction, resulting in ion accumulation inside the channel. Continuous and large ionic current can thus be maintained. However, under reverse bias, both cations and anions in the electric double layer are driven away from the junction, resulting in concentration depletion in the nanotube, and an energy barrier across the junction and the ionic current decrease. Figure 4c shows ionic current rectification behaviors at low and intermediate KCl bulk concentration.

Figure 4d shows the dependence of rectification ratio on the concentration of bulk KCl solution. The device shows slight rectification behavior at low ion concentration ($\leq 10^{-4}$ M) with the rectification ratio siting steadily at ~ 2. The diode characteristic becomes more evident at intermediate ion concentration and peaks at $\sim 3 \times 10^{-3}$ M, beyond which the rectification ratio drops quickly back to ~ 2 and continues to decrease until it goes back to the bulk bipolar behavior at high ionic strength. This trend tends to agree with the prediction from the solution of the full 2D Poisson−Nernst−Planck equations.[14] The reduced rectification at low ion concentration could be partially attributed to the concentration polarization at the entrance from the reservoirs to the nanotube. The potential bias between the two ends of the nanochannel becomes smaller than the bias applied between the two ends of reservoirs. Should this be the case, using a longer nanochannel would improve the device performance, since longer nanotubes should be less affected by the concentration polarization. Compared to the 5 μm long diode presented in Figure 4, a diode channel twice as long shows a distinct enhancement in the rectification ratio at low ionic strength (see Figure S6 in the Supporting Information), suggesting that concentration polarization is partially responsible for the reduced rectification ratio.[34]

Although the experimental trends qualitatively match with the theoretical prediction, the finite rectification ratios in these diode devices deviate from the ideal diode characteristics. Apart from increasing the channel length, further size reduction of such heterojunction nanotubes should also ensure better overlapping of electric double layer and result in a larger built-in potential at the junction and better diode performance.[14] In addition, a clean junction should enable better control over the ion and electric field distribution at the depletion area and such a clean junction has been adopted as an important boundary condition used in all fluidic diode simulations. We believe that by improving the junction sharpness, enhanced device performance should also be expected. The development of such nanofluidic devices would enable the modulation of ionic and molecular transport at a more sophisticated level and lead to large-scale integrated nanofluidic networks and logic circuits.

Acknowledgment. This work was supported by the Office of Basic Science, Department of Energy. P.Y. would like to thank NSF for the A.T. Waterman Award.

Supporting Information Available: Descriptions of heterojunction nanotube synthesis and nanotube diode device fabrication. This material is available free of charge via the Internet at http://pubs.acs.org.

References

(1) Goldberger, J.; Fan, R.; Yang, P. D. Inorganic nanotubes: A novel platform for nanofluidics. *Acc. Chem. Res.* **2006**, *39*, 239–248.
(2) Han, J. Y.; Fu, J. P.; Schoch, R. B. Molecular sieving using nanofilters: Past, present and future. *Lab Chip* **2008**, *8*, 23–33.
(3) Mijatovic, D.; Eijkel, J. C. T.; van den Berg, A. Technologies for nanofluidic systems: top-down vs. bottom-up - a review. *Lab Chip* **2005**, *5*, 492–500.
(4) White, H. S.; Bund, A. Ion current rectification at nanopores in glass membranes. *Langmuir* **2008**, *24*, 2212–2218.
(5) Martin, C. R.; Siwy, Z. S. Learning nature's way: Biosensing with synthetic nanopores. *Science* **2007**, *317*, 331–332.
(6) Dekker, C. Solid-state nanopores. *Nat. Nanotechnol.* **2007**, *2*, 209–215.
(7) Mannion, J. T.; Craighead, H. G. Nanofluidic structures for single biomolecule fluorescent detection. *Biopolymers* **2007**, *85*, 131–143.
(8) Fan, R.; et al. DNA translocation in inorganic nanotubes. *Nano Lett.* **2005**, *5*, 1633–1637.
(9) Tegenfeldt, J. O.; et al. Micro- and nanofluidics for DNA analysis. *Anal. Bioanal. Chem.* **2004**, *378*, 1678–1692.
(10) Sauer-Budge, A. F.; Nyamwanda, J. A.; Lubensky, D. K.; Branton, D. Unzipping kinetics of double-stranded DNA in a nanopore. *Phys. Rev. Lett.* **2003**, *90*, 238101.
(11) Daiguji, H.; Yang, P. D.; Majumdar, A. Ion transport in nanofluidic channels. *Nano Lett.* **2004**, *4*, 137–142.
(12) Fan, R.; Yue, M.; Karnik, R.; Majumdar, A.; Yang, P. D. Polarity switching and transient responses in single nanotube nanofluidic transistors. *Phys. Rev. Lett.* **2005**, *95*, 086607.
(13) Karnik, R.; et al. Electrostatic control of ions and molecules in nanofluidic transistors. *Nano Lett.* **2005**, *5*, 943–948.
(14) Daiguji, H.; Oka, Y.; Shirono, K. Nanofluidic diode and bipolar transistor. *Nano Lett.* **2005**, *5*, 2274–2280.
(15) Pennathur, S.; Eijkel, J. C. T.; van den Berg, A. Energy conversion in microsystems: is there a role for micro/nanofluidics. *Lab Chip* **2007**, *7*, 1234–1237.
(16) Gijs, M. A. M. Device physics - Will fluidic electronics take off. *Nat. Nanotechnol.* **2007**, *2*, 268–270.
(17) van der Heyden, F. H. J.; Bonthuis, D. J.; Stein, D.; Meyer, C.; Dekker, C. Electrokinetic energy conversion efficiency in nanofluidic channels. *Nano Lett.* **2006**, *6*, 2232–2237.

(18) Miedema, H.; et al. A biological porin engineered into a molecular, nanofluidic diode. *Nano Lett.* **2007**, *7*, 2886–2891.
(19) Alcaraz, A.; et al. A pH-tunable nanofluidic diode: Electrochemical rectification in a reconstituted single ion channel. *J. Phys. Chem. B* **2006**, *110*, 21205–21209.
(20) Vlassiouk, I.; Siwy, Z. S. Nanofluidic diode. *Nano Lett.* **2007**, *7*, 552–556.
(21) Karnik, R.; Duan, C. H.; Castelino, K.; Daiguji, H.; Majumdar, A. Rectification of ionic current in a nanofluidic diode. *Nano Lett.* **2007**, *7*, 547–551.
(22) Kalman, E. B.; Vlassiouk, I.; Siwy, Z. S. Nanofluidic bipolar transistors. *Adv. Mater.* **2008**, *20*, 293–297.
(23) Nishizawa, M.; Menon, V. P.; Martin, C. R. Metal Nanotubule Membranes with Electrochemically Switchable Ion-Transport Selectivity. *Science* **1995**, *268*, 700–702.
(24) Stein, D.; Kruithof, M.; Dekker, C. Surface-charge-governed ion transport in nanofluidic channels. *Phys. Rev. Lett.* **2004**, *93*, 035901.
(25) Coster, H. G. L. A Quantitative Analysis of Voltage-Current Relationships of Fixed Charge Membranes and Associated Property of Punch-Through. *Biophys. J.* **1965**, *5*, 669–686.
(26) Bassignana, I. C.; Reiss, H. Ion-Transport and Water Dissociation in Bipolar Ion-Exchange Membranes. *J. Membr. Sci.* **1983**, *15*, 27–41.
(27) Mafe, S.; Ramirez, P. Electrochemical characterization of polymer ion-exchange bipolar membranes. *Acta Polym.* **1997**, *48*, 234–250.
(28) Parfitt, G. D. Surface-Chemistry of Oxides. *Pure Appl. Chem.* **1976**, *48*, 415–418.
(29) Fan, R.; et al. Fabrication of silica nanotube arrays from vertical silicon nanowire templates. *J. Am. Chem. Soc.* **2003**, *125*, 5254–5255.
(30) Sjoback, R.; Nygren, J.; Kubista, M. Absorption and Fluorescence Properties of Fluorescein. *Spectrochim. Acta, Part A* **1995**, *51*, L7–L21.
(31) He, R. R.; et al. Si nanowire bridges in microtrenches: Integration of growth into device fabrication. *Adv. Mater.* **2005**, *17*, 2098–2102.
(32) Kosmulski, M. In *Encyclopedia of surface and colloid science*; Hubbard, A. T., Ed.; Marcel Dekker: New York, 2002; pp 1627−1636.
(33) Sprycha, R. Electrical Double-Layer at Alumina Electrolyte Interface 0.1. Surface-Charge and Zeta Potential. *J. Colloid Interface Sci.* **1989**, *127*, 1–11.
(34) Vlassiouk, I.; Smirnov, S.; Siwy, Z. Nanofluidic ionic diodes. Comparison of analytical and numerical solutions. *ACS Nano* **2008**, *2*, 1589–1602.

NL9020123